ChemPubSoc Europe

DOI: 10.1002/open.201900210

Open Access ChemistryOPEN Full Papers

Novel Conjugated Side Chain Fluorinated Polymers Based on Fluorene for Light-Emitting and Ternary Flash Memory Devices

Qian Zhang,[b] Dongge Ma,[c] Dianzhong Wen,[d] Cheng Wang,[e] Xuduo Bai,*[a] and Shuhong Wang*[a]

Three novel conjugated polymers based on 9,9′-dioctylfluorene unit and isoindolo[2,1-*a*]benzimidazol-11-one with different fluorine substituents (0, 2 and 4) were synthesized. PLED and resistive memory devices based on these polymers were prepared consequently. PLED based on four-fluorinated polymer showed the highest maximum brightness of 3192 cd m^{-2} with almost 5-fold increase of current efficiency 8-fold increase of external quantum efficiency compared to that of the other two, and all the PLEDs exhibited good emission stability with no noticeable change of electroluminescence even under high voltage of 10 V. The memory device of doubly-fluorinated polymer exhibited ternary flash behavior with threshold voltages below −2.5 V, while device of four-fluorinated polymer possessed ON/OFF current ratio above 10^4. Impact of fluorine substitutions on the performance of devices were briefly investigated. The results revealed that the improvement of device performance might not scale with the increasing number of fluorine substitutions, and the four-fluorine-substituted polymer and doubly-fluorinated polymer could be encouraging materials for applications of PLED and resistive memory device and worth of further design of other new polymer systems.

1. Introduction

The study of polymer light-emitting diodes (PLEDs) has been in progress ever since the discovery of their promising electroluminescent properties.[1] Compared to the inorganic and small molecular organic materials, conjugated polymers for light-emitting devices have many advantages such as the feasibility of large-surface manufacture by simply spin coating, low-costing, and the possibility for modifying polymers at the molecular level to tune the performances of device.[2] Among those polymers, polyfluorene and their derivatives have been widely studied as PLED materials because of the encouraging performance such as high photoluminescence quantum efficiency in the solid state, good thermal stability, good film forming properties, and the ease of modification at molecule level to achieve the balance of transport of carriers that may enhance the light emitting performances. Apart from various functional groups, polymers with halogen atoms (particularly the fluorine atom) substituted directly to the backbone as light emitting materials have been fairly reported, since the electron-withdrawing fluorine would lower the energy level of polymer, thus affect the emission. The impact of fluorine incorporation has been mainly discussed on the performance of photovoltaic cells,[3] and more work focus on backbone fluorinated polymers other than on side chain fluorinated ones. Based on the information above, we chose an isoindolo[2,1-*a*]benzimidazole–11-one structure[4] with different numbers of fluorine substituent (0, 2, 4) to copolymerize with a well processable 9,9′-dioctylfluorene, therefore, novel conjugated polymers of non-fluorinated polymer (PF0f) and sidechain-fluorinated polymers (PF2f, PF4f) are prepared for further study of their optoelectronic properties.

Conductive polymers used for resistive memory behaviors have attracted increasing interest due to their advanced physical and chemical properties such as highly mechanical flexibility, longer data retention time and low power consumption compared to the traditional semiconductor-based memory materials.[5] In the case of an asymmetric memory device, the configuration can be the same as that of a single-layer PLED (ITO/polymer/metal for instance), besides, the on-voltage of a

[a] *Prof. X. Bai, Prof. S. Wang*
School of Chemistry Engineering and Materials Science
Heilongjiang University
74 Xuefu Road, Nangang District, Harbin, China, 150080
E-mail: xuduobai@hotmail.com
openair@163.com
[b] *Q. Zhang*
School of Chemistry Engineering and Materials Science
Heilongjiang University
74 Xuefu Road, Nangang District, Harbin, China, 150080
[c] *D. Ma*
Institute of Polymer Materials
South China University of Technology
381 Wushan Road, Tianhe District, Guangzhou, China, 510641
[d] *D. Wen*
Key Laboratories of Senior-education for Electronic Engineering
Heilongjiang University
74 Xuefu Road, Nangang District, Harbin, China, 150080
[e] *C. Wang*
School of Chemistry Engineering and Materials Science
Heilongjiang University
74 Xuefu Road, Nangang District, Harbin, China, 150080

Supporting information for this article is available on the WWW under https://doi.org/10.1002/open.201900210

©2019 The Authors. Published by Wiley-VCH Verlag GmbH & Co. KGaA. This is an open access article under the terms of the Creative Commons Attribution Non-Commercial License, which permits use, distribution and reproduction in any medium, provided the original work is properly cited and is not used for commercial purposes.

flash-type memory device and a PLED could be within a quite close range.[6] A dual functional device requires careful fabrication and choose of suitable materials. For instance, Buket Bezgin Carbas et al.[7] have proposed a fluorene-based polymer with good dual electroluminescence and electrochromic properties, but the engineering of an electrochromic device and a PLED is quite different. Since the configuration of PLED and memory device can be the same, investigation of materials with dual light-emitting and resistive memory behavior are next step work. However, examples of fluorene-based polymer are rare in literature. In the light of above information, we also prepared resistive memory devices based on PF0f, PF2f and PF4f and investigate the memory switching performance to pave the way for further research to achieve dual function in one device.

2. Results and Discussion

2.1. Synthesis and Characterization of Polymer PF0f, PF2f and PF4f

To minimize the effects of sidechains on the optical properties of polymers and to investigate the impact caused by the fluorine substitutions, the same main structure was used for copolymerization. The general procedure of synthesis was shown in Scheme 1.

2.2. Poly[2,7-(9,9′-dioctylfluorene)-co-benzo[4,5]imidazo [2,1-*a*]isoindol-11-one] (PF0f)

0.279 g (0.5 mmol) of 9,9-dioctylfluorene-2,7-diboronic acid bis (1,3-pro-panediol) ester, 0.189 g (0.5 mmol) of 6,9-dibromobenzo[4,5]imidazo[2,1-*a*]isoindol-11-one (0f), 17 mg of $Pd(PPh_3)_4$ and 8 mL of toluene were used to afford 0.164 g of purified yellow green solid PF0f (53.9%). FT-IR (KBr, cm^{-1}): 714.3, 770.8, 814.3, 884.5, 938.9, 1069.9, 1123.9, 1177.7, 1256.2, 1276.1, 1310.9, 1415.6, 1464.5, 1481.7, 1606.0, 1755.5, 1781.7, 2851.9, 2925.1, 3057.5. ^{1}H NMR (400 MHz, $CDCl_3$), δ (ppm): 7.43–8.01 (m, 10 H, Ar H), 1.96–2.11 (m, 6 H, CH_2), 1.14–1.26 (m, 22 H, CH_2), 0.80–0.82 (m, 6 H, CH_3). ^{13}C NMR (100 MHz, $CDCl_3$), δ (ppm): 14.10, 22.62, 27.50, 29.37, 30.25, 40.36, 54.91, 55.14, 62.02, 119.18, 119.58, 120.06, 122.86, 127.92, 131.47, 132.40, 134.43, 140.87, 143.57, 147.42, 150.33, 151.63.

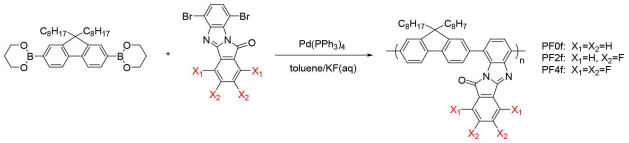

Scheme 1. Synthesis route of polymers PF0f, PF2f and PF4f.

2.3. Poly[2,7-(9,9′-dioctylfluorene)-co-2,3-difluorobenzo[4,5] imidazo[2,1-*a*]isoindol-11-one] (PF2f)

0.279 g (0.5 mmol) of 9,9-dioctylfluorene-2,7-diboronic acid bis (1,3-pro-panediol) ester, 0.207 g (0.5 mmol) of 2,3-difluoro-6,9-dibromobenzo[4,5]imidazo[2,1-*a*]isoindol-11-one (2f), 17 mg of $Pd(PPh_3)_4$ and 6 mL of toluene were used to afford 0.198 g of purified yellow green solid PF2f (61.5%). FT-IR (KBr, cm^{-1}): 726.8, 816.1, 890.2, 1123.0, 1275.5, 1314.4, 1414.0, 1464.7, 1483.8, 1607.1, 1770.3, 2852.7, 2925.6. ^{1}H NMR (400 MHz, $CDCl_3$), δ (ppm): 7.50–8.34 (m, 10 H, Ar H), 2.08–2.11 (m, 6 H, CH_2), 1.04–1.21 (m, 22 H, CH_2), 0.82–0.86 (m, 6 H, CH_3). ^{13}C NMR (100 MHz, $CDCl_3$), δ (ppm): 14.05, 22.59, 27.51, 30.22, 31.48, 35.37, 39.45, 55.52, 62.05, 116.16, 119.96, 120.71, 122.43, 123.42, 123.84, 125.88, 128.53, 128.85, 132.12, 141.82, 148.83, 151.50, 162.10.

2.4. Poly[2,7-(9,9′-dioctylfluorene)-co-1,2,3,4-tetrafluorobenzo [4,5]imidazo[2,1-*a*]isoindol-11-one] (PF4f)

0.279 g (0.5 mmol) of 9,9-dioctylfluorene-2,7-diboronic acid bis (1,3-pro-panediol) ester, 0.225 g (0.5 mmol) of 1,2,3,4-tetrafluoro-6,9-dibromobenzo[4,5]imidazo[2,1-*a*]isoindol-11-one (4f), 17 mg of $Pd(PPh_3)_4$ and 6 mL of toluene were used to afford 0.172 g of purified orange-yellow solid PF4f (50.6%). FT-IR (KBr, cm^{-1}): 719.1, 746.8, 816.1, 948.6, 1086.8, 1124.3, 1278.1, 1310.5, 1422.3, 1455.0, 1492.7, 1510.6, 1607.8, 1771.5, 2853.4, 2926.4. ^{1}H NMR (400 MHz, $CDCl_3$), δ (ppm): 7.55–8.31 (m, 10 H, Ar H), 1.98–2.11 (m, 6 H, CH_2), 1.13–1.27 (m, 22 H, CH_2), 0.80–0.82 (m, 6 H, CH_3). ^{13}C NMR (100 MHz, $CDCl_3$), δ (ppm): 14.06, 22.61, 23.69, 27.49, 29.28, 31.82, 40.33, 55.00, 62.06, 119.16, 119.52, 120.11, 124.00, 124.53, 126.80, 127.23, 127.89, 132.35, 143.17, 147.53, 150.32, 150.66.

In the case of IR spectrum, polymers exhibited similar characteristic bands around 2849–2918 cm^{-1} (strong C–H stretching for octyl chains), 1739 cm^{-1} (C=O stretching) and 1608–1466 cm^{-1} (C=C and C=N stretching). Note that the stretching vibrations of carbonyl groups in condensed cyclic γ-lactams would move to about 1760 cm^{-1} in their IR spectra.[4b] The C–F bonds don't usually possess a constant vibrational frequency nor do they always have unique absorption band features, which may lead to the difficulty of locating and recognizing their absorption.[8] Since the C–F stretching could exhibit two or more bands of polyfluorinated aliphatic hydrocarbons with a broad range of 1400–1000 cm^{-1},[8] and compared with the non-fluorinated monomer 0f, the aromatic C–F stretching bands of fluorinated monomer 2f and 4f were assumed to be (1471 cm^{-1},1486 cm^{-1}) and (1492 cm^{-1},1519 cm^{-1}), respectively. The C–F vibration of polymer PF2f was hard to recognize, and in terms of PF4f, the C–F stretching band could be located around 1510 cm^{-1}. The peak of ^{1}H NMR resonated in the region of 0.80-2.11 ppm and 7.43–8.34 ppm were assigned to the aliphatic and aromatic protons, respectively. The number of protons estimated from the integration of peaks agreed with the proposed structures. It's noticeable that two aromatic protons are eliminated due to the formation of new bond between the backbone of polymer.[9] In

© 2019 The Authors. Published by Wiley-VCH Verlag GmbH & Co. KGaA

the case of ^{13}C NMR, signal of carbon atom of C=O bond in isoindol-11-one units was easy to be effect by the heteroatom, thus the peak of this carbon could be observed around 159.5 ppm in PF0f (weak) and 162.1 ppm in PF2f, but hard to recognize in PF4f. The IR, ^{1}H NMR and ^{13}C NMR spectrum of polymers were all shown in supporting information (Figure S1 and S2).

2.5. Molecular Weight and Thermal Stability of Polymers

The molecular weights and thermal stability of prepared polymers of PF0f, PF2f and PF4f were listed in Table 1. The gel-permeation chromatography (GPC) trace and thermogravimetric analyses (TGA) were supplied in supporting information (Figure S3 and S4). All polymers showed good thermal stability with decomposition temperature above 300 °C and carbonized residue in nitrogen atmosphere above 30% at 600 °C. The molecular weights and thermal properties of polymers could well meet the requirements of spin-coating thin-layers in fabricating process of device.

2.6. Theoretical Quantum Calculation of Polymers

The molecular simulation based on the repeat unit of PF0f, PF2f and PF4f were carried out by hybrid density functional theory B3LYP/6-31 G basis set of Gaussian 09 program in order to get more insight into the properties of the polymers (Figure 1). The highest molecular orbital (HOMO) was not just located on the fluorene segment but on the whole backbone of the polymer, while the lowest unoccupied molecular orbital (LUMO) were located on the isoindolo[2,1-*a*]benzimidazol-11-one unit. The calculated HOMO energy levels of were −5.58 eV, −5.71 eV and −5.75 eV, while LUMOs were −2.55 eV, −2.86 eV and −3.17 eV, respectively. Introducing fluorine had more impact on the LUMOs of three polymers than HOMOs. which agreed with the electro-withdrawing natural of fluorine. However, the calculated dipole moment of PF0f, PF2f and PF4f were 2.57, 1.66 and 2.61 Debye respectively. The doubly-fluorinated polymer didn't possess the moderate but the smallest dipole moment among the three polymers. The dipole moment didn't follow the trend as fluorine substitution increasing which suggested that the number of fluorine substituents and the properties of the three polymers may not relate necessarily in a linear scale.

Table 1. Molecular weights of PF0f, PF2f and PF4f and their thermal properties.

	M_n	M_w	PDI	T_d (°C) [a]	carbonized residue (%) [b]
PF0f	13720	16752	1.22	341	32.7
PF2f	14430	17040	1.18	317	37.2
PF4f	13070	16270	1.24	350	39.2

[a] Decomposition temperature. [b] at 600 °C in nitrogen.

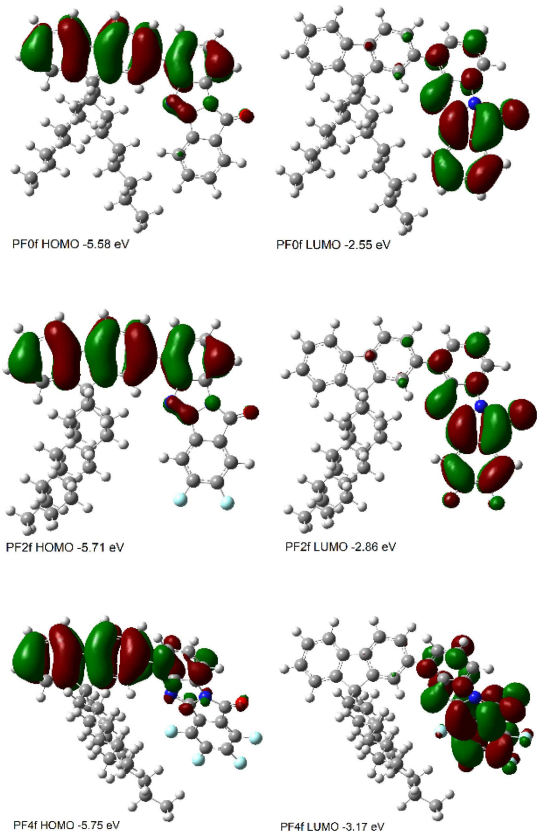

Figure 1. Electronic density contours of molecular orbitals of the repeated unit of PF0f.

2.7. Optical and Electrochemical Characteristics of Polymers

Figure 2a showed the absorption of PF0f, PF2f and PF4f in solution of THF and in solid films. The absorption of PF0f and PF2f were similar in shape with higher-energy band that could be assigned to π-π* transition of benzo[4,5]imidazo[2,1-*a*] isoindol-11-one segment around 320–340 nm[4a] and lower-energy but more intense band around 395 nm that could be assigned to π-π* transition along the main chain. The absorption of PF4f in solid state exhibited more extended tails near the edge that suggest stronger interchain interaction.[2a] No more typical absorption of all three polymers in solution and in films were observed, which indicated there may not be effective intramolecular charge transfer in ground state, which could be verified by DFT since the HOMOs and LUMOs of three polymers were located separately. High twist angles in main chain (about 40° of PF0f and PF2f) and in side chain (about 150° of PF0f and PF2f, 139° of PF4f) of three polymers were found according to the optimized geometries by theoretically calculation (Figure S5), which suggested the conformational distortion of polymers, thus restricted the charge transfer between fluorene unit and benzo[4,5]imidazo[2,1-*a*]isoindol-11-one segment.[10]

The effect of fluorine substitution on photoluminescence (PL) may not be in the same direction as on absorption. Red-shift of fluorinated polymer with respect to the non-fluorinated

© 2019 The Authors. Published by Wiley-VCH Verlag GmbH & Co. KGaA

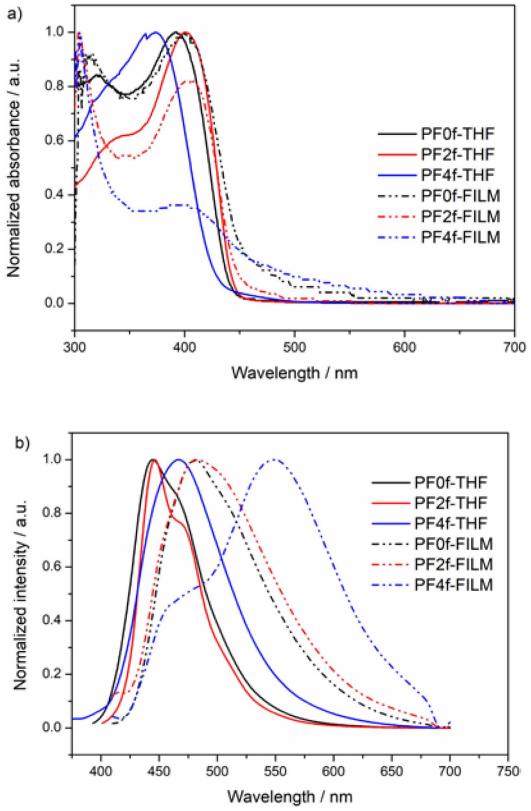

Figure 2. a) Normalized UV absorption of PF0f, PF2f and PF4f in THF and solid films, b) PL spectrum of PF0f, PF2f and PF4f in THF and solid films.

analogues could be observed in PL while absorption showed blue-shift.[3a] The PL spectrum of three polymers in solution and in films (Figure 2b) were similar except the PL of PF4f in solid state, which the blue emission band was weakened and a new dominated green emission that around 551 nm was exhibited. The less twist angle and more coplanar linkage between fluorene unit and the benzo[4,5]imidazo[2,1-*a*]isoindol-11-one segment of PF4f (8°, see Figure S4) may lead to the interchain aggregation, which may cause the new emission of 551 nm and result in more efficient excitation energy transfer that facilitated by intra- and interchain interaction of PF4f.[11]

The HOMO energy level was estimated from the formula $E_{HOMO} = (E\text{onset ox vs Ag/AgCl} + 4.4)$ eV, where *E*onset ox represented the onset of oxidation potential of each polymer in solid state that measured by cyclic voltammetry using 0.1 M tetra-*n*-butylammonium perchlorate in acetonitrile as electrolyte (Figure S6). The HOMO levels of PF0f and PF2f were approximated, and the LUMO levels were more affected by the presence of fluorine. The optical and electrochemical results (Figure 2 and Table 2) suggested that despite the strong electron-withdrawing nature of fluorine, the properties of these three polymers and their further behavior in devices may not scale with the increasing fluorine substituents.

2.8. Characteristics of Electroluminescence Device

PLEDs based on the three polymers were fabricated with the configuration of ITO/PEDOT: PSS/polymer/TPBi/LiF/Al. LiF was deposited on Al as cathode with work function of 3.1 eV. The benzo[4,5]imidazo[2,1-*a*]isoindol-11-one structure was electron deficient, which was expected to improve the electron transport ability once incorporated with the fluorene segment. Since the hole transporting was much higher than electron transporting in polyfluorene,[12] a hole block layer of 1,3,5-tris(N-phenyl-benziphenylbenzimidazol-2-yl) benzene (TPBi) was used to achieve the charge balance and enhance the performance of PLED devices,[13] as the barrier between the HOMO energy level of polymers and TPBi (−6.2 eV) was about 0.7 eV, which may confine the hole injection within the polymer layer. The *V-I-B* characteristics of devices (Figure 3a-b and Table 3) showed that bright emission at 11.8 V with the maximum brightness of 3192 cd m^{-2} was observed in PLED device based on PF4f, and the corresponding external quantum efficiency was 1.19% (Figure 3c), which was almost 8-fold increase by the EQE of the other two devices. The much better performance of PLED based on PF4f may attribute to the more coplanar structure, which could facilitate the charge transport through the backbone of

Table 2. Optical and electrochemical characteristics of PF0f, PF2f and PF4f.

	λ Abs.max (nm)		Abs.λonset (nm) [a]	PLmax (nm)[b]		*E*opt g(eV) [c]	E_{HOMO} (eV)	E_{LUMO} (eV) [d]
	Sol.	Film		Sol.	Film			
PF0f	393	401	463	445	481	2.72	−5.49	−2.77
PF2f	400	405 ± 4	457	446	484	2.78	−5.45	−2.67
PF4f	374	395 ± 9	492	467	461, 551	2.43	−5.56	−3.13

[a] Estimated from absorption edge of polymers in films. [b] Excited at 390 nm. [c] $E_g^{opt} = 1240/\text{Abs.}\lambda_{onset.}$ [d] $ELUMO = E_g^{opt} - E_{HOMO.}$

Table 3. Electroluminescence characteristics of PLEDs based on PF0f, PF2f and PF4f with active area of 0.16 cm^2.

	λEL^{max} (nm)	V_{on} (V)	CD^{max} (mA cm^{-2})	Bri.^{max} (cd m^{-2})	CE^{max} (cd A^{-1})	PE^{max} (lm W^{-1})	EQE^{max} (%)
PF0f	470 ± 12	4.8	548.9	379	0.35	0.23	0.14
PF2f	466 ± 10	3.4	601.0	642	0.29	0.26	0.13
PF4f	576 ± 12	4.6	404.7	3192	1.90	1.06	1.19

© 2019 The Authors. Published by Wiley-VCH Verlag GmbH & Co. KGaA

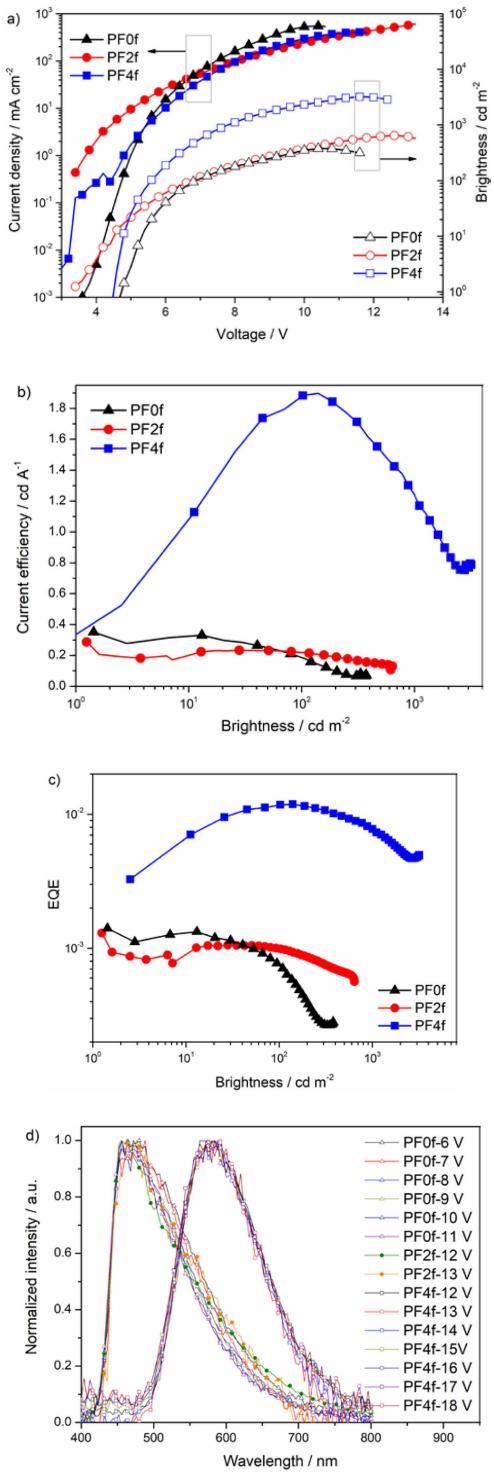

Figure 3. a) *V–I-B* performance, b) current efficiency, c) EQE and d) voltage dependence of normalized EL spectra of PLED devices based on PF0f (triangular symbol), PF2f (circular symbol) and PF4f (square symbol).

PF4f. The electroluminescent (EL) spectra (Figure 3d) of PF0f and PF2f were similar in shape and exhibited close maximum emission band around 470 nm. Compared with the PL, the blue emission around 460 nm was largely suppressed in EL of PF4f, indicating that the four-fluorinated-benzo[4,5]imidazo[2,1-*a*]isoindol-11-one units was efficient exciton traps.[11a] All devices possessed electroluminescent stability with no noticeable emission change under high voltages. The problems of broad emission and color purity affected from green emission which may due to the interchain interactions or keto-defect formation of polyfluorene backbone required to be addressed by further modification of polymer molecules and/or adding active layers in device to overcome the defect and to improve the performance of the PLEDs.

2.9. Characteristics of Memory Device

The memory devices based on PF0f, PF2f and PF4f as resist layers were fabricated with the simple structure of ITO/polymer/Al configuration (Figure 4), along with the scanning electron microscopic images (SEM) of polymeric layer. With the thickness around 68 nm, the surface of polymer was uniformed.

The memory behavior was investigated by current-voltage (*I–V*) characteristics, which the value of current was replotted on a log scale (Figure 5a–c). Take device based on PF0f (Figure 5a) for example, the first sweep under the voltage ranged from 0 to −6 V exhibited an OFF-to-ON transition which was defined as a "writing" process. With the increase applied bias during the first sweep, the current showed a sudden jump at −1.6 V, which revealed device switching from a low conductive state (OFF state) to a high conductive state (ON state). The device remained at the ON state during the whole second sweep, which was considered as a "reading" behavior of the device. With the applied bias reversed, the device exhibited an ON-to-OFF transition which was defined as an "erasing" process. The device remained at ON state until the applied bias increased to 3.7 V, then the current dropped sharply and the device switched back to OFF state. During the last sweep, the OFF state was sustained and the process was defined as "re-reading". The rewritable and nonvolatile four-stepped switching process revealed a flash type of memory device with an ON/OFF current ratio greater than 10^3.

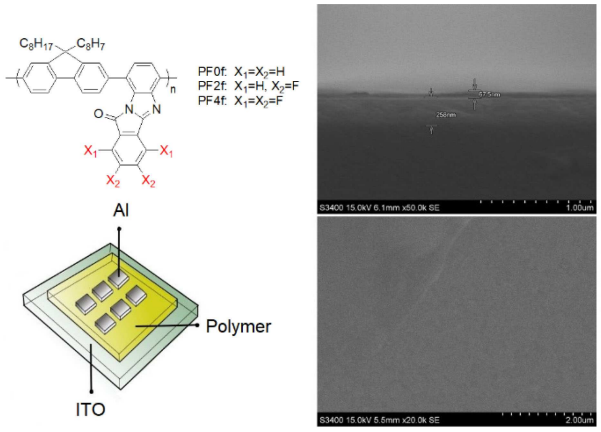

Figure 4. Illustration and SEM images of the ITO/polymer/Al memory device.

© 2019 The Authors. Published by Wiley-VCH Verlag GmbH & Co. KGaA

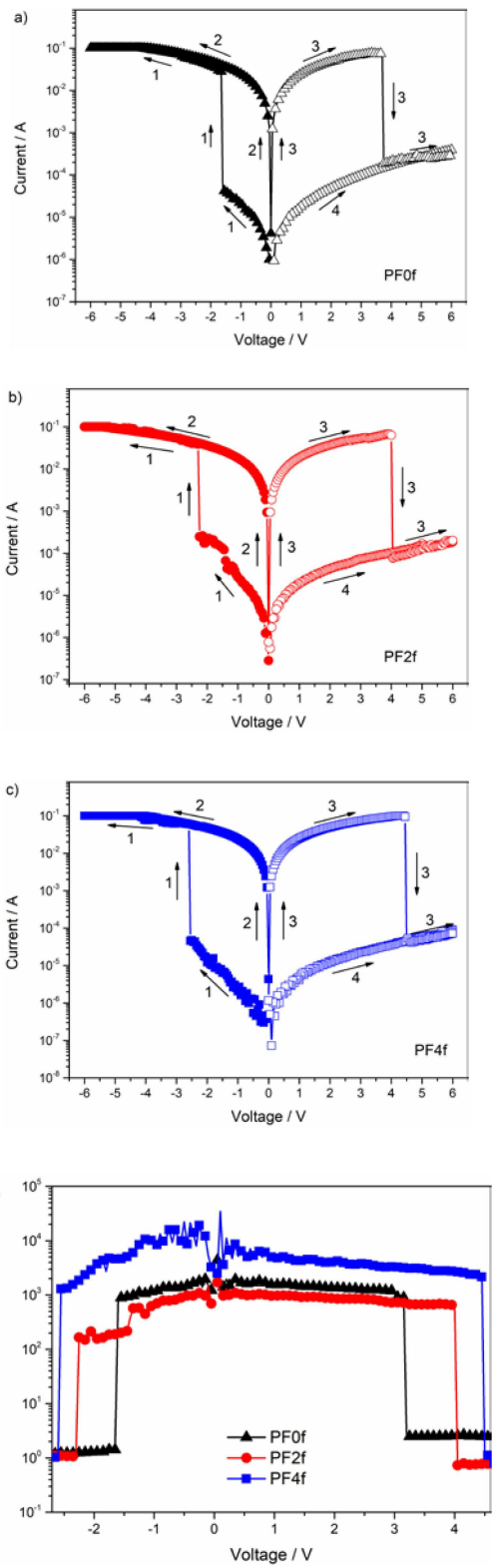

Figure 5. Current-voltage (*I–V*) characteristics of the ITO/Polymer/Al memory device based on a) PF0f, b) PF2f and c) PF4f, and d) ON/OFF ratio of three memory devices.

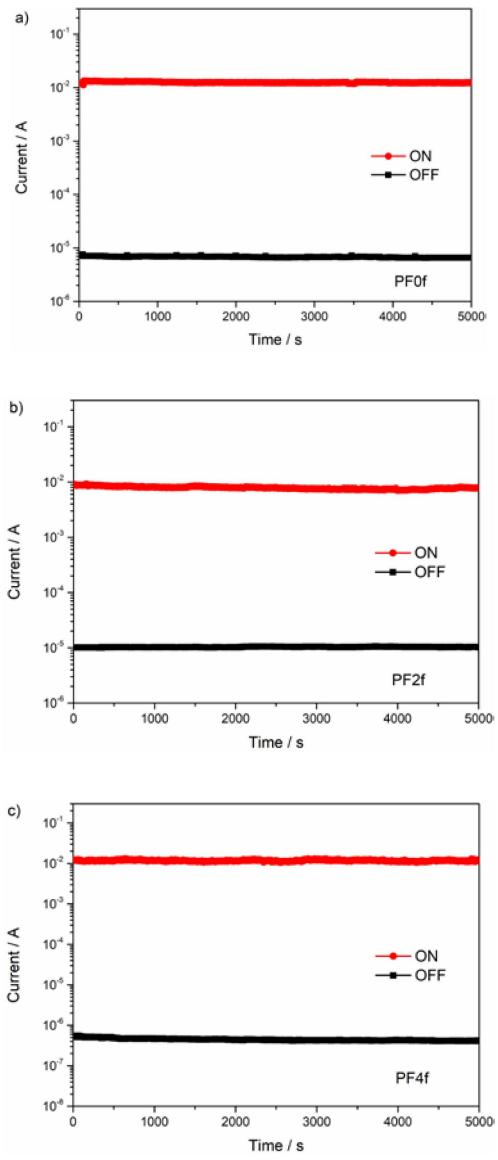

Figure 6. Retention behaviours under constant stress of −0.5 V of (a) PF0, (b) PF2 and (c) PF4.

The memory devices based on PF2f and PF4f exhibited similar flash behavior. In the second voltage scan from 0 V to −6 V, the current of two devices jumped to ON state under −2.2 V and −2.5 V, respectively. While in the third voltage scan from 0 to 6 V, the current of two devices sharp dropped to OFF state under 4 V and 4.5 V, respectively. Compared to the device based on PF0f, device with PF2f possessed a lower ON/OFF ratio that around 103, while device based on PF4f possessed much higher ON/OFF ratio that could reach to 10^4 (Figure 5d). Figure 6 showed the retention behaviors of the OFF and ON states of polymer memory devices. Under the constant stress of −0.5 V, no obvious degradation of these devices was observed for at least 5000 s.

One of the most widely used mechanisms of resistive memory devices based on conjugated polymer is the charge trapping/detrapping effect.[10,14] Figure 7 was the illustration of the molecular electrostatic potential (ESP, also MEP) of optimized structure of three dimers, where the positive regions

© 2019 The Authors. Published by Wiley-VCH Verlag GmbH & Co. KGaA

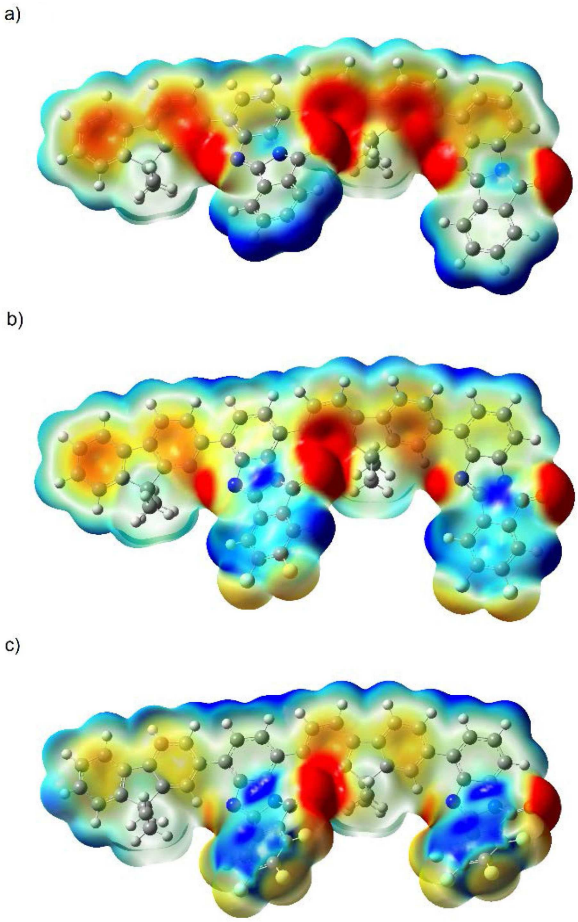

Figure 7. Electrostatic potential of optimized geometry of dimers of a) PF0f, b) PF2f and c) PF4f.

appeared as blue and negative regions as red. According to the definition of ESP, positive charges approaching molecule would favor the negative region, the more electron-rich sites, and vice versa.[15] Thus, holes and electrons injected from electrodes would be trapped by the negative and positive regions respectively. When applied voltages reached to threshold, the accumulated charges in the traps would lead to a sudden current jump from low conductive OFF state to high conductive ON state, and could be maintained due to the barriers of back-transfer.[14b] As Shown in Figure 7, all three polymers exhibited multiple traps that mostly located around the fluorene backbone and the oxygen and fluorine atom of isoindole segment. Within a repeat unit of polymer, one pair of hole and electron traps was observed for PF0f and PF4f while two pairs of traps for PF2f. The double-trap structure of PF2f may resulted in a ternary memory behavior (Figure 5b) since the carriers could filled the second pair of traps and lead to a second switching from ON 1 state to ON 2 state. All captured charges maintained until the reverse voltage was applied, which supplied enough energy to extract/detrap the trapped charges and turn the devices to initial OFF state, resulting in a nonvolatile flash behavior.

The *I–V* fitting curves of memory device based on three polymers were presented for further understanding of the switching behavior from OFF state to ON state under applied voltages (Figure 8). Take device of PF0f as example, at the beginning of charge injection from electrodes, the *I–V* curve of OFF state (Figure 8a) exhibited linear under lower voltage, which indicated the working mechanism followed ohmic conduction model as $J \propto V$ and the device was at a high resistance state.[14b,16] As applied voltage increasing, the current raised slowly and the *I–V* curve changed from ohmic to space charge limited conduction (SCLC) model as $J \propto V^2$[17] since the behavior of device was controlled by trapped carriers in this process as discussed above. After a sudden jump of current at on-voltage, the device switched from OFF state to ON state (Figure 8b) and dominated by the ohmic conduction again. Memory device of PF4f exhibited similar *I–V* curve region (Figure 8e–f). Since the PF2f device exhibited a ternary switching behavior, the *I–V* curve possessed one more region that fitted SLCL model (Figure 8c). All devices at ON state fitted the ohmic conduction quite well.

3. Conclusions

Three fluorene based conjugated polyfluorene polymers consisting of imidazo[2,1-*a*]isoindol-11-one moieties with comparable number of fluorine substitutions (0, 2 and 4) were synthesized and investigated. Introducing fluorine to side chain could noticeably change the optical, electrochemical properties of polymers and as well as key factors of light-emitting and memory devices, but the change may not scale with the number of fluorine substitution increasing, at least in our studied series (PF0f, PF2f and PF4f). The polymers with doubly fluorinated segment as PF2f showed the lowest on voltage of 3.4 V yet the medium brightness and EQE in PLED device, and lower ON/OFF ratio in flash memory device than that of non-fluorinated polymer (PF0f). On the other hand, four-fluorinated polymer PF4f exhibited the highest maximum brightness of 3192 cd m^{-2}, almost 5-fold increase of current efficiency and 8-fold increase of EQE in light-emitting device than that of the other two. Besides, PF2f was the only one exhibited ternary memory behavior among the three polymers. Considered that fluorine was substituted to side chain other than directly into the backbone of polymer, the performance of devices might be affected by various contribution instead of the sole effect of strong electron-withdrawing nature of fluorine. The results indicated that the electroluminescent performance and memory behaviors could be tuned by introducing fluorine substituents. The promising four-fluorine-substituted polymer PF4f, which possessed more improved PLED device parameters, and doubly fluorinated polymer PF2f, which possessed ternary flash memory behavior, could be considered for further use for other new polymer systems and for further modification of both display and memory storage applications.

© 2019 The Authors. Published by Wiley-VCH Verlag GmbH & Co. KGaA

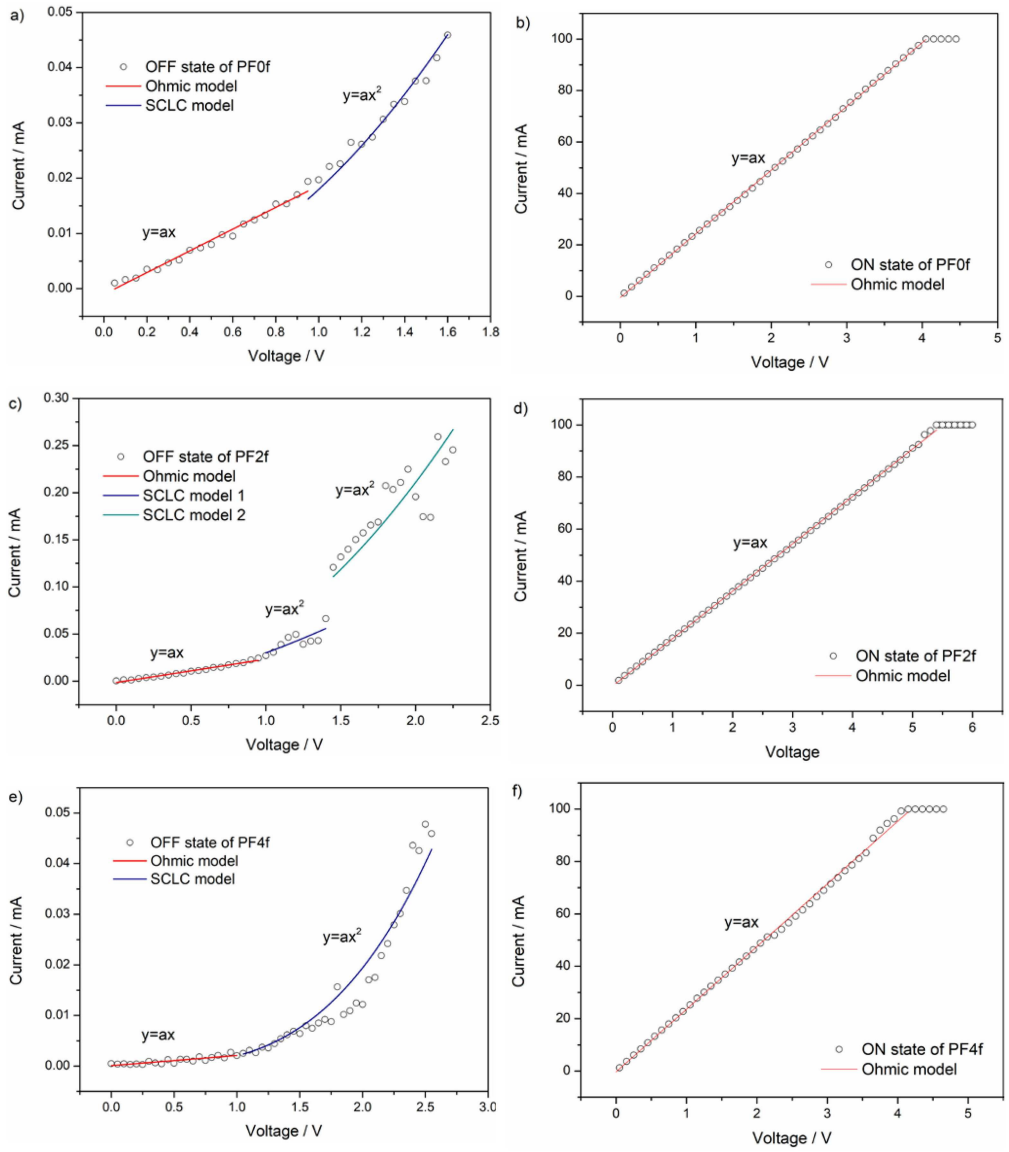

Figure 8. Experimental *I–V* curves (hollow circular symbol) and fitting *I–V* curves (solid line) of memory device based on PF0f (a, b), PF2f (c, d) and PF4f (e, f).

Experimental Section

Materials and Instruments

3,6-dibromobenzene-1,2-diamine and phthalic anhydride were purified by sublimation (10^{-2} mbar) before use. All other purchased chemicals were used as received. ITO substrates were well cleaned and treated by Photo Surface Processor (PL 16-110, replace lamp SUV110GS-36) before use. IR spectra were obtained from Perkin Elmer Spectrum 100 Model FT-IR spectrometer. ^{1}H NMR spectra were obtained on Bruker AC-400 MHz NMR Spectrometer. GPC analysis was recorded by using a Malvern instrument connected with Viscotek-VE3580-RI-Detector and standard polystyrene samples as calibration, which were performed on a polymer/THF solution at a flow rate of 1 mL min^{-1} at 30 °C. TGA were taken under nitrogen atmosphere with 10 °C min^{-1} rate and were recorded on Perkin Elmer Pyris 6 workstation. Photochemical measurements were obtained by using SHIMADZU UV-3600 and Jasco FP-6200 spectrophotometer. Cyclic voltammeter was measured by CHI-660E electrochemical workstation at a voltage scan rate of 50 mV s^{-1}. Luminance properties of PLED were recorded by using Keithley source measurement (Keithley 2400 and Keithley 2000) with a calibrated silicon photodiode. The electroluminescent spectra were obtained by using Spectra scan PR650 spectrophotometer. Memory behaviour was carried out by Keithley 4200-SCS semiconductor workstation under applied voltage with step of 0.05 V.

General Synthesis Procedure of Monomers and Polymers

The general synthesis procedure using *o*-phenylenediamine to prepare isoindolo[2,1-*a*]benzimidazole–11-one and its analogues have been fairly reported.[4] We chose the typical conditions of heating 3.6-dibromo-1,2-phenylenediamine and phthalic anhydride with different number of fluorines (0, 2, 4) under the reflux in acetic acid and acetic anhydride successively to prepare isoindolo[2,1-*a*]-6,9-dibromobenzimidazol-11-one ("0f"), 2,3-difluoroisoindolo[2,1-*a*]-6,9-dibromobenzimidazol-11-one ("2f") and 1,2,3,4-tetrafluoroisoindolo [2,1-*a*]-6,9-dibromobenzimidazol-11-one ("4f"). IR and ^{1}H NMR were used to verify the structural characterization of the three

© 2019 The Authors. Published by Wiley-VCH Verlag GmbH & Co. KGaA

monomers, which were described in Figure S7, along with the details of synthesis (Figure S6).

9,9-dioctylfluorene-2,7-diboronic acid bis(1,3-pro-panediol) ester, monomer, $Pd(PPh_3)_4$ (3 mol% based on total monomer) were dissolved in 6–8 mL of toluene and 1 mL of 2 M KF, degassed, backfilling with nitrogen and heated to reflux under N_2 atmosphere for 48 h. The resulting mixture was cooled to room temperature and extracted from toluene 3 times, concentrated to a small amount and re-precipitated from 180 mL of methanol/H_2O (8:1, v/v). The precipitate was collected, washed with acetone for 48 h by Soxhlet extraction, and finally dried under vacuum.

Device Preparation

The PLED devices were fabricated with the configuration of ITO/PEDOT: PSS/polymer/TPBi/LiF/Al. PEDOT: PSS was spin-coated on top of the ITO substrates at 1000 rpm for 1 min and dried at 80 °C for 1 h. Polymers solved in THF as 10 mg mL^{-1} solutions were then spin-coated above the PEDOT: PSS layer at 1500 rpm for 1 min. TPBi, LiF and Al were deposited under high vacuum of 1×10^{-6} mbar with a shadow mask to give the device an active area of 16 mm^2. Preparation steps after spin coating PEDOT: PSS were carried out in two interconnected N_2-filled glove boxes ($[O_2]<$ 3 ppm, $[H_2O]<0.5$ ppm). The memory devices were fabricated with the configuration of ITO/polymer/Al. Polymers in 10 mg mL^{-1} dichlorobenzene solution were spin coated on top of ITO substrates at 500 rpm for 1 min and dried at 80 °C under nitrogen. The samples were transferred to a thermal evaporation chamber with a shadow mask for Al deposition under high vacuum of 2×10^{-6} mbar

Acknowledgements

This research was supported by the National Natural Science Foundation of China (Grant no. 21372067, no. 51527804), the Doctoral Fund of Ministry of Education of China (Grant no. 20132301110001) and the Natural Science Foundation of Heilongjiang Province (Grant no. B2017010).

Conflict of Interest

The authors declare no conflict of interest.

Keywords: conducting polymers · fluorene-fluorinated polymer · polymer light emitting diodes · flash memory devices · ternary memory

[1] a) J. H. Burroughes, D. D. C. Bradley, A. R. Brown, R. N. Marks, K. Mackay, R. H. Friend, P. L. Burns, A. B. Holmes, *Nature* **1990**, *347*, 539–541; b) Y. Ohmori, M. Uchida, K. Muro, K. Yoshino, *Jan. J. App. Phys.* **1991**, *30*, L1941-L1943; c) R. M. Gurge, A. M. Sarker, P. M. Lahti, B. Hu, F. E. Karasz, *Macromolecules* **1997**, *30*, 8286–8292; d) A. Kraft, A. C. Grimsdale, A. B. Holmes, *Angew. Chem.* **1998**, *110*, 416–443; *Angew. Chem. Int. Ed.* **1998**, *37*, 402–428; e) A. C. Grimsdale, K. L. Chan, R. E. Martin, P. G. Jokisz, A. B. Holmes, *Chem. Rev.* **2009**, *109*, 897–1091; f) J. Liang, S. Zhao, X.-F. Jiang, J. T. Guo, H.-L. Yip, L. Ying, F. Huang, W. Yang, Y. Cao, *ACS Appl. Mater. Interfaces* **2016**, *8*, 6164–6173; g) J. Zhou, G. Fu, Y. He, L. Ma, W. Li, W. Feng, X. Lu, *J. Lumin.* **2019**, *209*, 427–434; h) R.-S. Sergio, L.-H. Luis-Abraham, M. Jose-Luis, C. Ramon, R.-O. Gabriel, P.-G. Enrique, S. Ullrich, G. Z. Mikhail, *Polymer* **2016**, *8*, 43, 1–12; i) J.-Y. Lin, B. Liu, M.-N. Yu, X.-H. Wang, L.-B. Bai, Y.-M. Han, C.-J. Ou, L.-H. Xie, F. Liu, W.-S. Zhu, X.-W. Zhang, H.-F. Ling, P. N. Stavrinou, J.-P. Wang, D. D. C. Bradley, W. Huang, *J. Mater. Chem. C* **2018**, *6*, 1535–1542.

[2] a) W.-C. Wu, C.-L. Liu, W.-C. Chen, *Polymer* **2006**, *47*, 527–538; b) H.-Y. Chen, C.-T. Chen, C.-T. Chen, *Macromolecules* **2010**, *43*, 3613–3623; c) X. Gao, Y. Zhang, C. Fang, X. Cai, B. Hu, G. Tu, *Org. Electron.* **2017**, *46*, 276–282; d) L. Bai, B. Liu, Y. Han, M. Yu, J. Wang, X. Zhang, C. Ou, J. Lin, W. Zhu, L. Xie, C. Yin, J. Zhao, J. Wang, D. D. C. Bradley, W. Huang, *ACS Appl. Mater. Interfaces* **2017**, *9*, 37856–37863; e) J. Lin, B. Liu, M. Yu, X. Wang, Z. Lin, X. Zhang, C. Sun, J. Cabanillas-Gonzalez, L. Xie, F. Liu, C. Ou, L. Bai, Y. Han, M. Xu, W. Zhu, T. A. Smith, P. N. Stavrinou, D. D. C. Bradley, W. Huang, *Adv. Mater.* **2019**, *31*, 1804811.

[3] a) I.-N. Kang, H.-K. Shim, T. Zyung, *Chem. Mater.* **1997**, *9*, 746–749; b) A. C. Stuart, J. R. Tumbleston, H. Zhou, W. Li, S. Liu, H. Ade, W. You, *J. Am. Chem. Soc.* **2013**, *135*, 1806–1815; c) M. Losurdo, M. M. Giangregorio, P. Capezzuto, G. Bruno, F. Babudri, A. Cardone, C. Martinelli, G. M. Farinola, F. Naso, M. Buchel, *Polymer* **2008**, *49*, 4133–4140; d) S. C. Price, A. C. Stuart, L. Yang, H. Zhou, W. You, *J. Am. Chem. Soc.* **2011**, *133*, 4625–4631.

[4] a) M. Mamada, C. Perez-Bolivar Jr., P. Anzenbacher, *Org. Lett.* **2011**, *13*, 4882–4885; b) E. V. Gromachevskaya, A. V. Finko, A. V. Butin, K. S. Pushkareva, V. D. Strelkov, L. I. Isakova, G. D. Krapivin, *Chem. Heterocycl. Compd.* **2013**, *49*, 1331–1344.

[5] a) B. Cho, S. Song, Y. Ji, T.-W. Kim, T. Lee, *Adv. Funct. Mater.* **2011**, *11*, 2806–2829; b) W. Lin, S. Liu, T. Gong, Q. Zhao, W. Huang, *Adv. Mater.* **2014**, *26*, 570–606; c) Y. Chen, G. Liu, C. Wang, W. Zhang, R.-W. Li, L. Wang, *Mater. Horiz.* **2014**, *1*, 489–506; d) J.-W. Choi, H.-C. Yu, J. Lee, J. Jeon, J. Im, J. Jang, S.-W. Jin, K.-K. Kim, S. Cho, C.-M. Chung, *Polymer* **2018**, *10*, 901, 1–12; e) H.-J. Yen, C. Shan, L. Wang, P. Xu, M. Zhou, H.-L. Wang, *Polymer* **2017**, *9*, 25 1–16.

[6] a) J. Liu, J. Cao, S. Shao, Z. Xie, Y. Cheng, Y. Geng, L. Wang, X. Jing, F. Wang, *J. Mater. Chem.* **2008**, *18*, 1659–1666; b) Y. Yang, L. Yu, Y. Xue, Q. Zou, B. Zhang, L. Ying, W. Yang, J. Peng, Y. Cao, *Polymer* **2014**, *55*, 1698–1706; c) Y. Zhang, L. Hu, J. Xu, R. He, J. Liang, F. Peng, W. Yang, Y. Cao, *Org. Electron.* **2018**, *61*, 366–375; d) Q. Ling, F. Chang, Y. Song, C. Zhu, D. Liaw, D. S. Chan, E. Kang, K. Neoh, *J. Am. Chem. Soc.* **2006**, *128*, 8732–8733; e) B. Zhang, Y.-L. Liu, Y. Chen, K.-G. Neoh, Y.-X. Li, C.-X. Zhu, E.-S. Tok, E.-T. Kang, *Chem. Eur. J.* **2011**, *17*, 10304–10311 f) Y. Liu, N. Li, X. Xia, J. Ge, Q. Xu, J. Lu, *Eur. Polym. J.* **2011**, *47*, 1160–1167.

[7] B. B. Carbas, D. Asil, R. H. Friend, A. M. Onal, *Org. Electron.* **2014**, *15*, 500–508.

[8] The Sadtler Handbook of Infrared Spectra, in: Sadtler Spectral Handbooks, Bio-Rad Laboratories, Inc., Informatics Division.

[9] M. Fukuda, K. Sawada, K. Yoshino, *J. Polym. Sci. Part A* **1993**, *31*, 2465–2471.

[10] H.-C. Wu, C.-L. Liu, W.-C. Chen, *Polym. Chem.* **2013**, *4*, 5261–5269.

[11] a) Z. Liu, L. Wang, J. Chen, F. Wang, X. Ouyang, Y. Cao, *J. Polym. Sci. Part A* **2007**, *45*, 756–767; b) M. S. Liu, J. Luo, A. K. Y. Jen, *Chem. Mater.* **2003**, *15*, 3496–3500; c) C. Ou, N. J. Cheetham, J. Weng, M. Yu, J. Lin, X. Wang, C. Sun, J. Cabanillas-Gonzalez, L. Xie, L. Bai, Y. Han, D. D. C. Bradley, W. Huang, *iScience* **2019**, *16*, 399–409; d) W. Shi, Z. Zhang, S. Li, *J. Phys. Chem. Lett.* **2018**, *9*, 373–382; e) J.-Y. Lin, B. Liu, M.-N. Yu, C.-J. Ou, Z.-F. Lei, F. Liu, X.-H. Wang, L.-H. Xie, W.-S. Zhu, H.-F. Ling, X.-W. Zhang, P. N. Stavrinou, J.-P. Wang, D. D. C. Bradley, W. Huang, *J. Mater. Chem. C* **2017**, *5*, 6762–6770.

[12] a) M. Redecker, D. D. C. Bradley, *Appl. Phys. Lett.* **1998**, *73*, 1565–1567; b) A. Babel, S. A. Jenekhe, *Macromolecules* **2003**, *36*, 7759–7764.

[13] a) L. Ying, J. Zou, W. Yang, A. Zhang, Z. Wu, W. Zhao, Y. Cao, *Dyes Pigm.* **2009**, *82*, 251–257; b) U. Giovanella, C. Botta, F. Galeotti, B. Vercelli, S. Battiato, M. Pasini, *J. Mater. Chem. C* **2013**, *1*, 5322–5329.

[14] a) S. Miao, H. Li, Q. Xu, Y. Li, S. Ji, N. Wang, J. Zheng, J. Lu, *Adv. Mater.* **2012**, *24*, 6210–6215; b) H.-C. Wu, A.-D. Yu, W.-Y. Lee, C.-L. Liu, W.-C. Chen, *Chem. Commun.* **2012**, *48*, 9135–9137.

[15] V. P. Gupta, in *Principles and Applications of Quantum Chemistry*, Chapter 6, Academic Press, Elsevier Inc. **2016**, pp. 195–214.

[16] Y.-Q. Li, R.-C. Fang, A.-M. Zheng, Y.-Y. Chu, X. Tao, H.-H. Xu, S.-J. Ding, Y.-Z. Shen, *J. Mater. Chem.* **2011**, *21*, 15643–15654.

[17] D. S. Shang, Q. Wang, D. Chen, R. Dong, X. M. Li, W. Q. Zhang, *Phys. Rev. B* **2006**, *73*, 245427–1-245427-7.

Manuscript received: June 12, 2019
Revised manuscript received: September 16, 2019

© 2019 The Authors. Published by Wiley-VCH Verlag GmbH & Co. KGaA